Phospholamban Binds in a Compact and Ordered Conformation to the Ca-ATPase†

Jinhui Li, Yijia Xiong, Diana J. Bigelow, and Thomas C. Squier*

Cell Biology Group, Department of Biological Sciences, Fundamental Sciences Division, Pacific Northwest National Laboratory, Richland, Washington 99352

Received August 10, 2003; Revised Manuscript Received November 8, 2003

ABSTRACT: Mutagenesis and cross-linking measurements have identified specific contact interactions between the cytosolic and the transmembrane sequences of phospholamban (PLB) and the Ca-ATPase, and in conjunction with the high-resolution structures of PLB and the Ca-ATPase, have been used to construct models of the PLB-ATPase complex, which suggest that PLB adopts a more extended structure within this complex. To directly test these predictions, we have used fluorescence resonance energy transfer to measure the average conformation and heterogeneity between chromophores covalently bound to the transmembrane and cytosolic domains of PLB reconstituted in proteoliposomes. In the absence of the Ca-ATPase, the cytosolic domain of PLB assumes a wide range of structures relative to the transmembrane sequence, which can be described using a model involving a Gaussian distribution of distances with an average distance (R_{av}) of less than 21 Å and a half-width (HW) of 36 Å. This conformational heterogeneity of PLB is consistent with the 10 structures resolved by NMR for the C41F mutant of PLB in organic cosolvents. In contrast, PLB bound to the Ca-ATPase assumes a unique and highly ordered conformation, where $R_{av} = 14.0 \pm 0.3$ Å and HW $= 3.7 \pm 0.6$ Å. The small spatial separation between the bound chromophores on PLB is inconsistent with an extended conformation of bound PLB in current models. Thus, to satisfy known interaction sites of PLB and the Ca-ATPase, these findings suggest a reorientation of the nucleotide binding domain of the Ca-ATPase toward the bilayer surface to bring known PLB binding sites into close juxtaposition with residues near the amino-terminus of PLB. Induction of an altered conformation of the nucleotide binding domain of the Ca-ATPase by PLB binding is suggested to underlie the reduced calcium sensitivity associated with PLB inhibition of the pump.

Phospholamban (PLB)[1] is coexpressed with the Ca-ATPase in cardiac and slow-twitch skeletal muscle and associates with the Ca-ATPase to modulate the calcium transient by reducing the calcium sensitivity of the pump (*1*, *2*). Phosphorylation of PLB by cAMP-dependent protein kinase (PKA) following β-adrenergic stimulation releases the inhibitory interaction between PLB and the Ca-ATPase, resulting in accelerated rates of muscle relaxation and greater cardiac force generation (*3*−*5*). Modulation of the inhibitory interaction between PLB and the Ca-ATPase, therefore, represents a major focus of therapies aimed at rescuing the failing heart (*5*−*8*). However, a rational development of antagonists that disrupt the inhibitory interaction between PLB and the Ca-ATPase requires an understanding of the structural interaction and mechanism of inhibition.

Cross-linking and mutagenesis measurements coupled with high-resolution structures of PLB and the Ca-ATPase provide important insights regarding the inhibitory interaction between PLB and the Ca-ATPase and have been interpreted to suggest that inhibition requires PLB to adopt an extended structure (*9*−*14*). Prior to association with the Ca-ATPase, the cytosolic (residues 4−16) and transmembrane (residues 22−49) helical domains of PLB are connected through either a β- or a flexible-turn linker (Figure 1), which functions as a hinge element permitting the cytosolic domain of PLB to adopt a range of conformations relative to the transmembrane domain (*9*, *15*−*17*). Alterations in the structure of this linker region connecting the transmembrane and cytosolic domains of PLB have been detected upon association with the Ca-ATPase and are suggested to function as a part of a conformational switch to modulate the inhibitory interaction between PLB and the Ca-ATPase (*17*−*19*). There are no significant changes in the backbone-fold of PLB upon association with the Ca-ATPase (*20*), suggesting that alterations in the arrangement of the transmembrane and cytosolic helical elements may play a critical role in modulating Ca-ATPase function. However, a complete understanding of the regulatory interactions between PLB and the Ca-ATPase requires that the structural interaction between these proteins be identified, as well as global changes within the backbone-fold of both proteins resulting from their association.

† This work was supported by a grant from the National Institutes of Health (HL64031).

* Corresponding author. E-mail: thomas.squier@pnl.gov. Tel: (509) 376-2218. Fax: (509) 376-1494.

[1] Abbreviations: ATP, adenosine 5′-triphosphate; cAMP, adenosine 3′:5′-cyclic monophosphate; CCCP, carbonyl cyanide 3-chlorophenyhydrazone; $C_{12}E_9$, polyoxyethylene-9-lauryl ether; EGTA, ethylene glycol-bis(β-aminoethyl ether)-*N*,*N*,*N*′,*N*′-tetraacetic acid; OG, *n*-octyl β-D-glucopyranoside; PKA, cAMP-dependent protein kinase; PLB, phospholamban; PMal, *N*-1-pyrenyl maleimide; POPOP, 1,4-bis [5-phenyl-2-oxazolyl]-benzene; SDS, sodium dodecyl sulfate; SDS−PAGE, sodium dodecyl sulfate−polyacrylamide gel electrophoresis; SERCA, sarco(endo)plasmic Ca-ATPase; SR, sarcoplasmic reticulum; TNM, tetranitromethane.

10.1021/bi035424v CCC: $27.50
Published on Web 12/20/2003

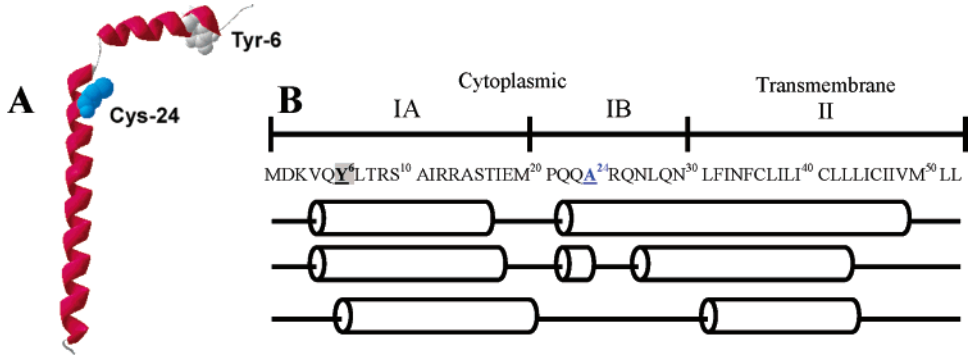

FIGURE 1: Depiction of backbone fold of PLB (A) (1FJK PDB) and its suggested helical content (B) (cylinders) before and after association with the Ca-ATPase. Relative positions of donor chromophore PMal (blue) covalently bound to position A24C and acceptor chromophore nitrotyrosine (grey) at position 6 are highlighted. The complete amino acid sequence of cytoplasmic (IA and IB) and transmembrane domains of PLB (B) is shown with the associated helical content (cylinders) measured from solid-state NMR for PLB alone (top; ref *9*) and from two models for PLB in association with the Ca-ATPase (middle, ref *13*; bottom, ref *14*).

To understand the binding interaction between PLB and the Ca-ATPase responsible for enzyme inhibition, we have measured the overall dimensions of the cytoplasmic portion of PLB following binding to the Ca-ATPase. Thus, using fluorescence resonance energy transfer (FRET), we have measured the spatial separation and conformational heterogeneity between donor and acceptor chromophores located at Tyr^6 near the amino-terminal end of the cytosolic region and at position 24 within the transmembrane domain of PLB following coreconstitution with the purified Ca-ATPase in membrane bilayers made from lipids extracted from sarcoplasmic reticulum (SR) membranes. These measurements demonstrate that PLB binds in a unique and highly ordered conformation to the Ca-ATPase. The donor−acceptor distance indicates a compact structure consistent with the average NMR structure of unbound PLB. These dimensions measured for the ATPase-bound form of PLB suggest that the nucleotide binding domain of the Ca-ATPase undergoes reorientation relative to the crystal structure of SERCA1 (i.e., 1IWO PDB; ref *12*) to bind PLB and satisfy constraints associated with known interaction sites on PLB and the Ca-ATPase.

EXPERIMENTAL PROCEDURES

Materials. *N*-(1-Pyrenyl)maleimide (PMal) was obtained from Molecular Probes, Inc. (Junction City, OR). Tetranitromethane (TNM) was purchased from Alrich (Milwaukee, WI). Polyoxyethylene 9 lauryl ether ($C_{12}E_9$), cAMP-dependent protein kinase (PKA), cAMP, ATP, $MgCl_2$, the calcium ionophore A23187, EGTA, DEAE-cellulose, and *n*-octyl β-D-glucopyranoside (OG) were purchased from Sigma (St. Louis, MO). 3-(*N*-Morpholino)propane-sulfonic acid (MOPS) was purchased from Fisher Biotech (Fair Lawn, NJ). Bio-Beads SM2 were purchased from Bio-Rad (Richmond, CA). Cardiac SR membranes were purified as previously described (*21*). Lipids were extracted from the SR vesicles isolated from rabbit skeletal fast-twitch muscle by standard methods (*22*, *23*). The Ca-ATPase was affinity purified from skeletal muscle SR using reactive Red-agarose (*24*). DNA encoding the single cysteine mutant PLB (PLB, $Cys^{36,41,46}/Ala^{24}Cys$) was cloned into a pGEX-2T plasmid expression vector and expressed in JM109 *Escherichia coli* cells as previously described (*17*, *25*). The concentration of PLB was determined by the Amido Black method (*26*). Affinity-purified PLB and Ca-ATPase were stored at −70 °C.

Coreconstitution of the Ca-ATPase with PLB. Before reconstitution, the anionic detergent SDS in the purified PLB sample obtained from preparative SDS−PAGE was exchanged for nonionic detergent $C_{12}E_9$ using DEAE-cellulose chromatography. This step involved the application of approximately 2 mg of purified PLB in 10 mL of buffer containing 20 mM MOPS (pH 7.0) and 2.5% $C_{12}E_9$ onto a DEAE-cellulose column preequilibrated with the same buffer. PLB was eluted with 20 mM MOPS (pH 7.0), 2.5% $C_{12}E_9$, and 0.2 M NaCl. PLB was reconstituted in the absence or presence of purified Ca-ATPase at a molar ratio of 1:2 PLB per Ca-ATPase into liposomes of extracted SR lipids as previously described (*27*). Thus, for activity measurements, two PLB were added per Ca-ATPase to ensure maximal inhibition (*2*, *28*). For fluorescence measurements, one PLB was added per Ca-ATPase, minimizing the likelihood of FRET between proximal PLB proteins bound to the Ca-ATPase and maximizing the amount of PLB bound to the Ca-ATPase since under these conditions 70 ± 6% of the PLB is associated with the Ca-ATPase (*2*, *20*).

Enzymatic, Protein, and Free Calcium Assays. ATP hydrolysis activity of the Ca-ATPase was determined by measuring the time course of the release of inorganic phosphate (*29*), using 100 μg of protein/mL in a solution containing 50 mM MOPS (pH 7.0), 0.1 M KCl, 5 mM $MgCl_2$, 1 mM EGTA, 1 μM CCCP, 2 μM valinomycin, 2 μM A23187, and sufficient calcium to yield the desired concentration of free calcium (*27*). To phosphorylate PLB for enzyme activity measurements, 10 μg PKA/mL and 1 μM cAMP were also included in the assay buffer, incubating the solution at 25 °C for 10 min before the addition of 5 mM ATP to start the reaction. All protein concentrations were determined by the Amido−Black method (*26*). Free calcium concentrations were calculated from total ligand and EGTA concentrations, correcting for pH and ionic conditions (*30*).

Specific Derivitization of PLB. The chemical modification of the single Cys^{24} with PMal and the nitration of the single Tyr^6 with tetranitromethane (TNM) was carried out as previously described (*17*). Before modification of Cys^{24} with PMal, PLB was incubated in the presence of 50 mM K_2PO_4 (pH 7.2), 50 mM DTT, and 0.1% $C_{12}E_9$ for 3 h at room

temperature. Following the separation of PLB from DTT using a Sephadex G-15 size-exclusion column, 6 μM PLB was incubated with 12 μM PMal in buffer A [50 mM K_2PO_4 (pH 7.2) and 0.1% $C_{12}E_9$] at 25 °C for 3 h. The reaction was quenched by the addition of 0.1 mM DTT before separating the labeled PLB from PMal using DEAE anion-exchange chromatography. After extensive washing, the bound PLB was eluted with buffer A containing 0.5 M NaCl. Incorporation of PMal was determined in buffer A using the molar extinction coefficient of $\epsilon_{343} = 3.6 \times 10^4$ M^{-1} cm^{-1} (*31*). For nitration of Tyr^6, 6 μM PLB was suspended in 0.1 M Tris (pH 8.0), 1 M NaCl, and 0.1% $C_{12}E_9$ before the addition of 24 μM TNM, which was incubated at 25 °C for 1 h. PLB was then separated into 10 mM Tris buffer (pH 8.0) using a Sephadex G-15 size-exclusion column. The extent of nitration was typically about 92% and was determined following solubilization in 10 mM Tris (pH 8.0), 0.5 M NaCl, and 0.1% $C_{12}E_9$ using the molar extinction coefficient of $\epsilon_{428} = 4200$ M^{-1} cm^{-1} (*32*).

Fluorescence Measurements. Steady-state fluorescence spectra were measured using a Spex Industries (Edison, NJ) Fluoromax-2 spectrofluorometer. Frequency domain data (lifetime and anisotropy) were measured using an ISS K2 frequency domain fluorometer (ISS Inc., Champaign, IL), as described previously (*33*). Excitation used the 333 nm output from a Coherent (Santa Clara, CA) Innova 400 argon ion laser; emitted light was collected after a Corion interference filter (50% transmittance at 400 nm; HW = 10 nm), using 1,4-bis[5-phenyl-2-oxazolyl]-benzene (POPOP) in methanol (lifetime of 1.35 ns) as a lifetime reference. Measurements were made at 25 °C.

Analysis of Frequency-Domain Data. Explicit expressions, previously described in detail, permit the ready calculation of the lifetime components (i.e., α_i and τ_i) relating to a multiexponential decay or the Gaussian distribution of distances between donor and acceptor chromophores (*33*−*38*). In the case of FRET measurements, the incomplete nitration of Tyr^6 was taken into account, as previously described (*39*). Alternatively, algorithms are available that permit the determination of the initial anisotropy in the absence of rotational diffusion (r_o), the rotational correlation times (φ_i), and the amplitudes of the total anisotropy loss associated with each rotational correlation time ($r_o g_i$), as previously described in detail (*40, 41*). The parameter values are determined using the method of nonlinear least-squares analysis in which the reduced chi-squared (i.e., χ_R^2) are minimized (*42*). A comparison of χ_R^2 values provides a quantitative assessment of the adequacy of different assumed models to describe the data (*43*). Data were fit using the Globals software package (University of Illinois, Urbana-Champaign) or the program Mathcad (MathSoft Inc., Cambridge, MA), where errors in measurements of the phase and modulation were respectively assumed to be 0.20 and 0.005.

RESULTS

Functional Reconstitution of Engineered and Derivatized PLB with the Ca-ATPase. A single cysteine mutant of PLB was constructed in which the three cysteines in the transmembrane sequence (Cys^{36}, Cys^{41}, and Cys^{46}) of wild-type PLB were substituted with alanines, and a further cysteine substitution was introduced (i.e., A24C) into the transmembrane sequence near the lipid−water interface to permit site-specific incorporation of a fluorescent probe at this position to assess the structure of PLB (Figure 1). Following its expression and purification, the PLB mutant was derivatized with the fluorophore *N*-(1-pyrenyl) maleimide (PMal), and Tyr^6 was nitrated with full retention of function, as previously described (*17*, *18*). The expressed and derivatized PLB is able to fully inhibit the Ca-ATPase, as evidenced by the equivalent calcium-dependent activation of the Ca-ATPase in comparison to native SR vesicles isolated from cardiac SR (Figure 2). Specifically, the calcium concentration necessary for one-half-maximal activation (i.e., $[Ca_{1/2}]$) for the reconstituted preparation ($[Ca_{1/2}] = 0.66 \pm 0.02$ μM) is virtually identical to that observed for cardiac SR ($[Ca_{1/2}] = 0.64 \pm 0.02$ μM) and upon release of the inhibitory interaction between PLB and the Ca-ATPase following addition of PKA, there is a similar shift in the calcium concentration dependence of activation toward lower calcium concentrations (i.e., $\Delta Ca_{1/2} = 0.3$ μM). Thus, measurements of the spatial separation between PMal and nitroTyr^6 will provide reliable information regarding the inhibitory interaction between PLB and the Ca-ATPase.

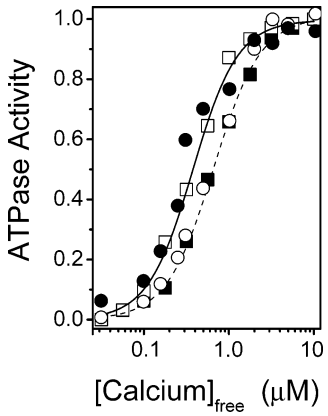

FIGURE 2: Calcium dependence of ATPase activity for the Ca-ATPase in native cardiac SR microsomes (○, ●) or following coreconstitution of the Ca-ATPase with mutant PLB following covalent attachment of PMal to Cys^{24} and nitration of Tyr^6 (■, □) in the absence (○, ■) or presence (●, □) of PKA. Calcium concentrations associated with half-maximal activation of the Ca-ATPase were 640 ± 30 nM (○), 660 ± 20 nM (■), 290 ± 30 nM (●), and 360 ± 20 nM (□). Coreconstituted samples have a molar ratio of 2 mol of PLB per mole of Ca-ATPase. The average maximal Ca^{2+}-dependent ATPase activity for these samples was, respectively, 7.2 ± 0.2 and 1.0 ± 0.1 μmol of P_i mg^{-1} min^{-1} at 25 °C for the Ca-ATPase coreconstituted with PLB and cardiac SR membranes and was not significantly affected by PKA addition.

Selective Measurement of PLB Bound to the Ca-ATPase. To assess the structure of PLB bound to the Ca-ATPase, we have taken advantage of the environmental sensitivity of the spectral shape and intensity of pyrene to modest differences in solvent polarity (*44*). For example, comparing PLB alone reconstituted in SR membranes with PLB following coreconstitution with the Ca-ATPase, there are significant increases in the relative intensities of the two major peaks, centered near 376 and 394 nm, with an average 3.6-fold increase in the fluorescence intensity of PMal-PLB (Figure 3). Thus, pyrene maleimide is sensitive to structural changes within PLB induced by its interaction with the Ca-ATPase, consistent with localized secondary structural changes between Ala^{24} and Glu^{26} in PLB as previously described (*18*, *19*). Further information regarding the dimensions of the

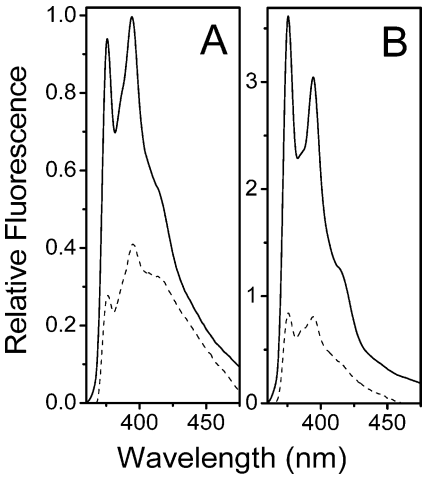

FIGURE 3: Fluorescence enhancement and increased fluorescence resonance energy transfer upon association between PLB and the Ca-ATPase. Steady-state emission spectra of PMal bound to Cys^{24} before (—) and following (- - -) nitration of Tyr^6 for PLB (4 μM) reconstituted in the absence (A) and presence (B) of the Ca-ATPase (2 μM). Experimental conditions involved either 24 μg/mL (A) or 250 μg/mL (B) total protein in 50 mM MOPS (pH 7.0), 0.1 M KCl, 5 mM $MgCl_2$, 70 μM $CaCl_2$, and 1 mM EGTA at 25 °C. λ_{ex} = 343 nm and bandwidth = 5 nm for both excitation and emission.

cytosolic domain of PLB is available using fluorescence resonance energy transfer (FRET), taking advantage of the large increase in the quantum yield of PMal-PLB upon binding to the Ca-ATPase to selectively monitor PLB bound to the Ca-ATPase. Using the reconstitution stoichiometries of this experiment (i.e., 2 mol of PLB added per mole of Ca-ATPase; Figure 3), approximately one-half of the total PLB is bound to the Ca-ATPase. Thus, there is an approximate 7-fold increase in the fluorescence quantum yield of PMal bound to Cys^{24} in PLB upon binding to the Ca-ATPase. For all subsequent fluorescence measurements, an equimolar ratio of PLB was coreconstituted with the Ca-ATPase. Under these latter conditions, approximately 70 ± 6% of the total PLB is bound in a functionally active form to the Ca-ATPase (*2*, *20*). Thus, more than 94% of the total fluorescence signal is associated with the population of PMal-PLB bound to the Ca-ATPase, permitting the selective measurement of PLB bound to the Ca-ATPase.

Dimensions of the Cytosolic Domain of PLB Bound to the Ca-ATPase. To assess the overall dimensions of PLB bound to the Ca-ATPase in lipid membranes, we have measured the decrease in the fluorescence intensity of PMal bound to Cys^{24} (FRET donor) following the selective nitration of Tyr^6 (FRET acceptor) (Figure 1A). Following nitration of Tyr^6, the intensity of the fluorescence emission spectrum of PMal-PLB, reconstituted in the absence and presence of the Ca-ATPase, respectively, decreases by approximately 60 and 80% (Figure 3). The increase in energy transfer efficiency observed in the presence of the Ca-ATPase is largely the result of the enhanced quantum yield of PMal, and the associated increase in the Förster distance (R_o) that defines the efficiency of energy transfer. Thus, the average spatial separation between PMal bound to Cys^{24} and nitroTyr^6 (as measured for bound PLB) is about 18 Å (Table 1), consistent with previous NMR measurements of PLB in organic cosolvents (1FJK PDB; ref *9*). These results suggest that the overall dimensions of the cytosolic domain of PLB are not significantly affected by association with the Ca-ATPase.

Fluorescence Lifetime Measurements. Complementary information concerning the conformation of PLB bound to the Ca-ATPase is available from a consideration of the time-dependent intensity decay of PMal measured using frequency-domain fluorescence spectroscopy, which permits the resolution of conformational heterogeneity that may underlie inhibition of the Ca-ATPase by PLB. For example, PLB may associate with the Ca-ATPase in multiple conformations, and the average FRET measured from the steady-state fluorescence intensity measurement may not reflect the bound conformation responsible for enzyme inhibition. In contrast, time-dependent measurements of the fluorescence decay permit the resolution of static quenching and conformational heterogeneity.

Frequency-domain fluorescence spectroscopy was used to measure the intensity decay of PMal bound to Cys^{24} in PLB in the absence and presence of nitroTyr^6 (Figure 4). Data were collected at 20 frequencies between 0.4 and 200 MHz. Upon increasing the frequency, there is a progressive increase in the phase and a decrease in the modulation. In comparison to PLB alone, the frequency-response is shifted toward lower frequencies upon PLB binding to the Ca-ATPase. These results indicate that the lifetime of PMal-PLB increases upon association with the Ca-ATPase, in agreement with the increased fluorescence intensity observed from the steady-state fluorescence measurements under similar conditions (Figure 3). Following nitration of Tyr^6 in PLB, the frequency-response of PMal-PLB is shifted to the right, indicating that the average lifetime is reduced because of the presence of FRET. However, in comparison to PLB reconstituted alone, the frequency-dependent shift is much larger following coreconstitution with the Ca-ATPase, confirming the steady-state measurements demonstrating the presence of greater FRET (Table 1). Indeed, there is good agreement between the energy transfer efficiency (*E*) calculated from the steady-state and lifetime data for PLB alone (i.e., $E = 52 \pm 8\%$ vs $58 \pm 15\%$) and following the reconstitution of PLB with the Ca-ATPase (i.e., $E = 82 \pm 13\%$ vs $78 \pm 3\%$) (Figure 3; Table 1). Assuming a single unique conformation of PLB, the decrease in average lifetime can be used to calculate an apparent spatial separation, which is approximately 18 Å (Table 1). These results are consistent with the steady-state fluorescence measurements and thus indicate that there is minimal static quenching, which would indicate a significant population of PLB conformations that bring nitroTyr^6 within 9−11 Å (i.e., 1/2 R_0) of PMal bound to Cys^{24}. Therefore, from this distance, it is apparent that the average structure of the cytosolic domain of PLB is very similar irrespective of its association with the Ca-ATPase, suggesting that binding to the Ca-ATPase does not involve large structural changes.

Conformational Heterogeneity of Cytosolic Domain of PLB. Additional information regarding the conformation of the cytosolic domain of PLB is available from fitting the time-dependent decays of PMal to a model that assumes a Gaussian distribution of distances between donor and acceptor chromophores (*34*, *37*, *45*). The intensity decay of PMal-PLB covalently bound to Cys^{24} can be adequately described as a sum of four exponentials, irrespective of its association with the Ca-ATPase, as indicated by the random distribution of the weighted residuals about the origin (Figure 4). Inclusion of additional fitting parameters results in no

Table 1: Energy Transfer and Spatial Separation between PMal Bound to Cys[24] and Tyr[6] [a]

experimental conditions	E[b] (%)	$\bar{\tau}_D$ (ns)	$\bar{\tau}_{DA}$ (ns)	R_o[c] (Å)	r_{app}[d] (Å)	R_{av}[e] (Å)	HW[e] (Å)	χ^2_R[f]
PLB	58 ± 15	5.4 ± 1.8	2.3 ± 0.3	19.1 ± 0.1	18 ± 2	<20.8	36 (18.6−42.8)	10.8
PLB + Ca-ATPase	78 ± 3	13.2 ± 0.4	2.9 ± 0.4	21.8 ± 0.1	17.7 ± 0.2	14.0 (13.8−14.3)	3.7 (3.1−4.3)	5.9

[a] Values and associated errors were obtained from three (SERCa) or six (PLB alone) independent measurements of FRET between PMal-Cys[24] and nitroTyr[6] in 50 mM MOPS (pH 7.0), 0.1 M KCl, 5 mM $MgCl_2$, 1 mM EGTA, and 70 μM $CaCl_2$ resulting in the presence of 30 nM free calcium, where the fractional nitration of Tyr[6] was typically approximately 0.92. [b] Energy transfer efficiencies (E) represent average values and associated standard errors of the mean calculated using lifetime measurements of PMal-Cys[24] (see the legend of Figure 4). [c] Förster critical distance (R_o) under the indicated experimental conditions represents the distance between chromophores where the FRET efficiency is 50% (*63*, *64*). [d] Apparent distance between PMal-Cys[24] and nitroTyr[6] calculated assuming a unique conformation. [e] Average donor−acceptor distance (R_{av}) or full-width at half-maximum (HW) assuming a Gaussian distribution of distances (*34*, *37*, *38*). Indicated errors were obtained from a global analysis of errors, as depicted in Figure 5. [f] Average value of reduced chi-squared (χ^2_R) fit to Gaussian distribution of distances.

further improvement in the goodness-of-fit. The similar goodness-of-fit (i.e., χ^2_R) obtained when fitting the lifetime data to a model that assumes a Gaussian distribution of distances with two floating parameters (i.e., R_{av} and HW; Table 1) in comparison to the fit obtained using a sum of exponentials with nine floating parameters (i.e., α_1, τ_1, α_2, τ_2, α_3, τ_3, and τ_4; see legend of Figure 4) indicates that fitting the data to the simpler model involving a distribution of distances is statistically justified.

The apparent spatial separation (r_{app}) calculated assuming a unique donor−acceptor separation is similar to the average spatial separation (R_{av}) determined from the distance distribution model, irrespective of the association of PLB with the Ca-ATPase (Table 1). A consideration of the error surfaces for these calculated distance distributions provides a conservative estimate of the recovered parameters (*46*) and demonstrates the presence of a well-defined conformation for the cytoplasmic domain of PLB following binding to the Ca-ATPase (Figure 5). In contrast to PLB alone, where the average spatial separation between chromophores is poorly determined (i.e., R_{av} <20.8 Å), the average distance between PMal at Cys[24] and nitroTyr[6] within bound PLB is precisely defined (i.e., R_{av} = 14.0 ± 0.3 Å; Figure 5). Furthermore, there are large differences in the calculated HW (full width at half-maximum height), which characterizes the width of the distribution. Prior to binding to the Ca-ATPase, the HW is 36 Å, indicating that the cytoplasmic domain of PLB adopts a wide distribution of conformations, consistent with the presence of a flexible hinge connecting cytoplasmic and transmembrane domains of PLB (*9*, *17*). However, following association with the Ca-ATPase, the cytoplasmic domain of PLB adopts a narrow conformational distribution (HW = 3.7 ± 0.6 Å) indicating that PLB binds in a unique conformation (Figure 6).

Fluorescence Anisotropy Measurements. To further assess possible changes in the structure of PLB associated with binding to the Ca-ATPase, we have measured the rotational dynamics of PMal covalently bound to Cys[24] in PLB using frequency-domain fluorescence anisotropy methods. These measurements resolve both the segmental rotational motion associated with PMal and changes in the global motions of the transmembrane domain of PLB. The differential phase and modulated anisotropy were measured over 20 frequencies between 0.4 and 200 MHz for PMal-PLB alone and following coreconstitution with the Ca-ATPase (Figure 7). One observes that there is a progressive increase in both the differential phase and the modulated anisotropy as the frequency increases. The overall shape of the frequency-responses for PLB in the absence and presence of the Ca-ATPase are very similar, indicating that the rates of motion are not significantly affected by association with the Ca-ATPase. Rather, the amplitudes associated with each rotational rate are affected, such that the contribution of faster motions associated with backbone fluctuations of PLB are reduced upon binding to the Ca-ATPase. This qualitative conclusion is reinforced from a quantitative consideration of the frequency responses of the differential phase and modulated anisotropy, which requires that the data be fit using the method of nonlinear least squares to a sum of exponentials. The fit to the frequency responses before and after the association of PLB with the Ca-ATPase requires a model involving two rotational rates and a residual anisotropy (Table 2), which are related to the independent motion of the probe (φ_1), dynamic fluctuations in the protein backbone (φ_2), and the extent of conformational restriction (anisotropic motion) imposed by the membrane bilayer and association with the Ca-ATPase on PLB (*27*). PMal does not detect any significant change in the backbone-fold of PLB (i.e., φ_2) following association with the Ca-ATPase. These results are consistent with earlier suggestions that Cys[24] is in a conformationally disordered region of PLB that does not undergo direct contact interactions with the Ca-ATPase (*18*, *19*, *47*). Thus, observed changes in the conformational heterogeneity between the cytosolic and the transmembrane domains of PLB measured using FRET reflect the stabilization of the cytosolic domain of PLB following association with the Ca-ATPase, rather than a global structural change involving the transmembrane domain. Furthermore, large amplitude motions of PMal are retained following association with the Ca-ATPase, which in conjunction with the fact that both PMal and nitroTyr[6] are solvent exposed, suggest that donor and acceptor chromophores are motionally averaged (i.e., $\kappa^2 = 2/3$) and that errors in the calculations of distances from the FRET measurements are no larger than 3 Å (*17*, *18*, *27*, *34*, *37*, *48*).

DISCUSSION

We have used FRET to measure the spatial separation and conformational heterogeneity between donor (D) and acceptor (A) chromophores, located respectively on the transmembrane and cytosolic domains of PLB (Figure 1), permitting a determination of the structure of PLB bound to the Ca-ATPase within lipid membranes. Specifically, the donor PMal was used to selectively label an introduced cysteine at position 24, near the cytosolic interface of the transmembrane domain of PLB. Nitration of Tyr[6], located

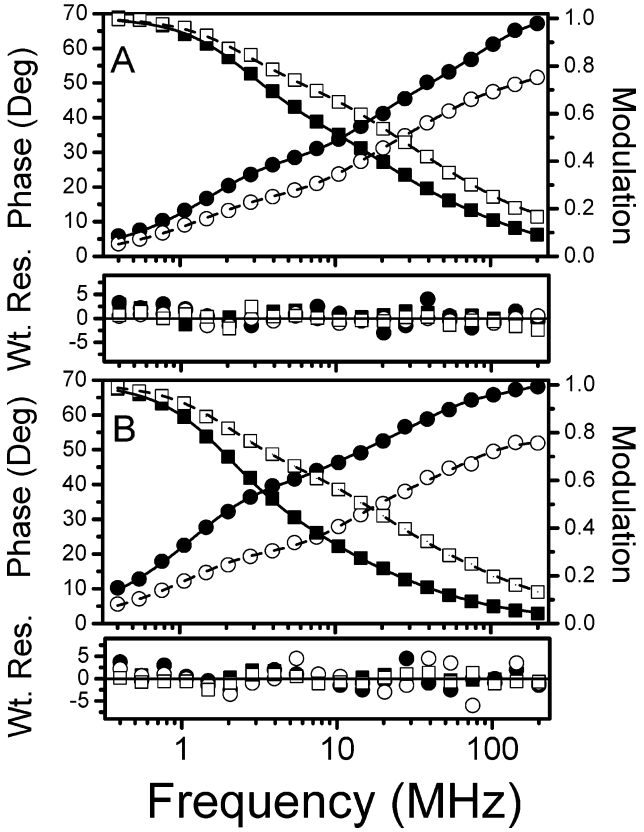

FIGURE 4: Frequency-domain lifetime data for PMal bound to PLB in the absence (A) and presence (B) of the Ca-ATPase. Frequency-response and four-exponential fits (solid and dashed lines) corresponding to the phase shift (●, ○) and modulation (■, □) for PMal-PLB in the absence (●, ■) and presence (○, □) of the FRET acceptor nitroTyr[6]. Measurements were made at 25 °C using 30 nM (0.2 μg/ml) PLB reconstituted with SR lipids in the absence (A) and presence of 30 nM (3 μg/mL) Ca-ATPase (B) in 50 mM MOPS (pH 7.0), 0.1 M KCl, 5 mM $MgCl_2$, 70 μM $CaCl_2$, and 1 mM EGTA, resulting in a free calcium concentration of approximately 30 nM (*30*). Data were fit to a sum of four exponentials, where $I(t) = \sum_i \alpha_i e^{-t/\tau i}$, and the mean lifetime ($\bar{\tau}$) was calculated as $\sum_i \alpha_i \tau_i$. Lower panels below respective data sets represent the weighted residuals (i.e., the difference between the experimental data and the calculated fit divided by the experimental uncertainty) for models involving four-exponential fit to the data. Calculated lifetime parameters for PMal (donor only) bound to Cys^{24} in PLB were (A) $\alpha_1 = 0.49 \pm 0.08$; $\tau_1 = 0.3 \pm 0.1$ ns; $\alpha_2 = 0.31 \pm 0.03$; $\tau_2 = 2.5 \pm 0.4$ ns; $\alpha_3 = 0.16 \pm 0.05$; $\tau_3 = 10 \pm 1$ ns; $\alpha_4 = 0.04 \pm 0.02$; $\tau_4 = 63 \pm 7$ and (B) $\alpha_1 = 0.45 \pm 0.01$; $\tau_1 = 0.5 \pm 0.1$ ns; $\alpha_2 = 0.28 \pm 0.01$; $\tau_2 = 4.2 \pm 0.4$ ns; $\alpha_3 = 0.17 \pm 0.01$; $\tau_3 = 16 \pm 1$ ns; $\alpha_4 = 0.10 \pm 0.01$; $\tau_4 = 95 \pm 1$ ns. The goodness-of-fit was calculated by minimizing the χ^2_R, which minimizes the sum of the differences between the calculated and the experimental values as previously described (*33*). For PMal-PLB reconstituted in the absence of the Ca-ATPase, $\chi^2_R = 4.9$ (donor only) and 1.4 (donor−acceptor). For PMal-PLB reconstituted in the presence of the Ca-ATPase, $\chi^2_R = 2.8$ (donor only) and 2.7 (donor−acceptor).

near the amino-terminus of the cytosolic domain, permits its use as a FRET acceptor to measure the conformation of the cytosolic domain of PLB. Following association with the Ca-ATPase, there is a large increase in the quantum yield of PMal (Figure 3), permitting the selective measurement of the structure of the bound PLB. Thus, these probes, which do not compromise the regulatory function of PLB (Figure 2), permit a determination of the structural changes in the backbone-fold of PLB associated with the binding and inhibition of the Ca-ATPase and a direct assessment of current structural models that suggests inhibition of the Ca-ATPase requires substantial changes in the secondary structure of PLB (Figure 1) (*13*, *14*).

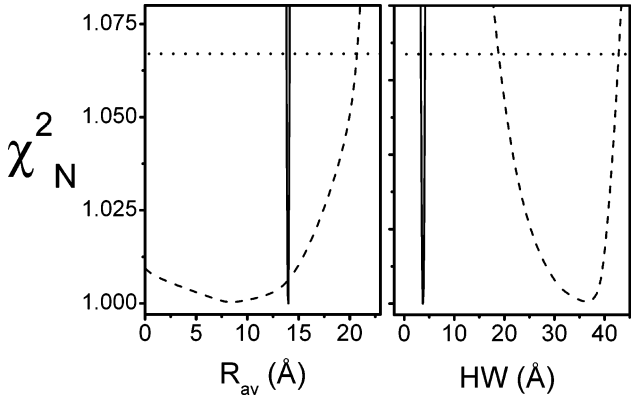

FIGURE 5: Depiction of error surfaces demonstrating disorder-to-order transition in the conformational heterogeneity of PLB upon binding to the Ca-ATPase. Experimental curves correspond to parameter values for average donor−acceptor separation (R_{av}) and associated half-width (HW) for a model involving a Gaussian distribution of the donor−acceptor distances. Error surfaces were obtained from a global fit for at least three data sets for PLB in the absence (dashed line) or presence (solid line) of the Ca-ATPase. Error surfaces were constructed by incrementally adjusting either R_{av} or HW and allowing all other parameters to vary in the least-squares analysis, which provides a conservative estimate of changes in the recovered values (*46*). The horizontal line corresponds to the *F* statistic for one standard deviation. Experimental conditions are as described in the legend of Figure 4.

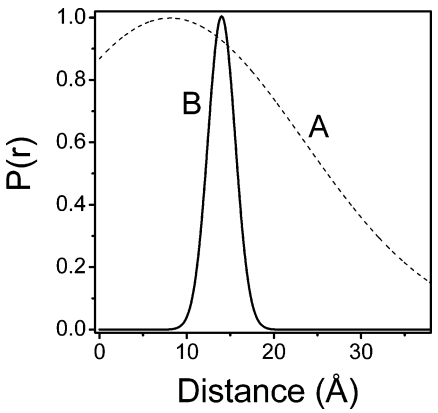

FIGURE 6: Decreased conformational hetrogeneity in the cytosolic domain of PLB upon association with the Ca-ATPase. Graphical depiction of peak-normalized Gaussian distance distributions depicting the relationship between the fractional population of donor−acceptor distances $P(r)$ and spatial separation r (distance) between PMal covalently bound to Cys^{24} and nitroTyr[6] in PLB reconstituted in the absence (A) and presence (B) of the Ca-ATPase. Experimental conditions are as described in the legend of Figure 4, where the average distance (R_{av}) and half-width (HW = 2.357φ) values that define the distance distribution model were determined from the rigorous analysis of errors depicted in Figure 5, where $P(r) = (\exp[-(1/2)(r - R_{av}/\sigma)^2]/P(r)_{max})$.

We report that prior to association with the Ca-ATPase, the cytosolic domain of PLB assumes a wide range of structures relative to the transmembrane sequence, which can be described using a model involving a Gaussian distribution of distances with an average distance (R_{av}) less than 21 Å and a half-width (HW) of 36 Å (Figures 5 and 6; Table 1). In contrast, PLB bound to the Ca-ATPase assumes a unique and highly ordered conformation, where $R_{av} = 14.0 \pm 0.3$ Å and HW = 3.7 ± 0.6 Å. The narrow range of conformations observed following binding to the Ca-ATPase, which

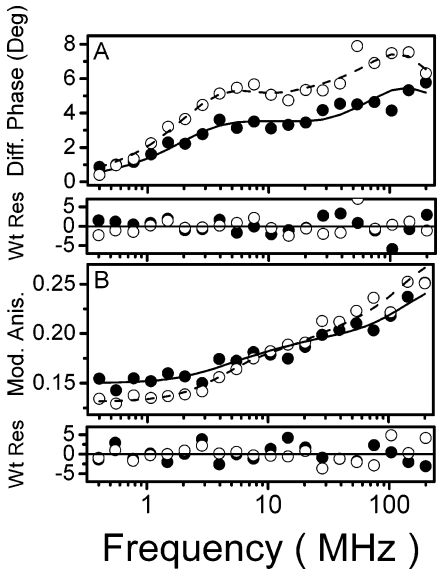

FIGURE 7: Rotational mobility of phospholamban. Fluorescence anisotropy decays for PMal-PLB in the presence (●, —) or absence (○, - - -) of the Ca-ATPase. Measured differential phase angles and modulated anisotropies (●, ○) and associated nonlinear least-squares fits to multiexponential model (—, - - -) where $r(t) = (r_o - r_\infty)\Sigma_{i=1}^{n} g_i \exp^{-(t/\phi_i)} + r_\infty$ and where r_o and r_∞ are the limiting anisotropy in the absence and presence of rotational diffusion, φ_i are the rotational correlation times, and $r_o g_i$ represent the amplitudes associated with the total anisotropy loss associated with each rotational correlation time. The weighted residuals (wt. res.) are shown below respective data sets. Experimental conditions are as described in the legend of Figure 4.

reflects both probe mobility and conformational heterogeneity in the backbone-fold of PLB, indicates a unique and homogeneous binding interaction between PLB and the Ca-ATPase. Since the average spatial separation between PMal at Cys^{24} and nitroTyr^6 does not significantly change (Table 1), these results in conjunction with earlier FTIR measurements that indicated that there are no large changes in the secondary structure of PLB upon association with the Ca-ATPase strongly suggest that there are no large changes in the secondary structure of PLB upon association with the Ca-ATPase (*20*). Rather, it is apparent that binding to the Ca-ATPase stabilizes a preexisting conformation of PLB.

The small spatial separation between the bound chromophores on PLB requires that to maintain known contact interactions between PLB and the Ca-ATPase, the orientation of the nucleotide binding domain of the Ca-ATPase moves toward the bilayer surface, in agreement with prior physical measurements that indicate a 9 ± 4° reorientation of the nucleotide binding domain of the Ca-ATPase following the release of PLB inhibition (*49*) (Figure 8). Thus, prior to PLB binding, large amplitude motions of the nucleotide binding domain of the Ca-ATPase are associated with the transport mechanism of the pump, and alterations in this catalytically important domain motion by PLB binding to the nucleotide binding domain, alterations in lipid fluidity and composition, or modulation through covalent cross-linking modulates calcium transport activity (*12*, *21*, *49*−*57*). Thus, it is the induction of an altered conformation of the nucleotide domain of the Ca-ATPase by PLB binding that modulates calcium activation of the Ca-ATPase and that would be expected to diminish the efficiency of ATP utilization and enzyme phosphorylation, which underlies the reduced calcium sensitivity associated with PLB inhibition of the pump.

Prior cross-linking and mutagenesis measurements have identified critical binding interfaces between PLB and the Ca-ATPase and have demonstrated that inhibition involves association between the transmembrane and the cytosolic domains of PLB and the Ca-ATPase. Specifically, Lys^3 in the cytosolic domain of PLB has been cross-linked by a 15 Å cross-linking reagent, to a sequence (i.e., $KDDKPVK^{402}$) within the nucleotide binding domain of the Ca-ATPase (*5*, *50*, *58*). Likewise, cysteine cross-linking reagents indicate proximal relationships between residues 27, 30, and 49 in PLB with, respectively, residues 321, 318, and 89 of the Ca-ATPase (*14*, *59*). These reagents place a 10−15 Å distance restraint on the relative position of PLB with respect to the pump and provide important constraints on the structural interface between the transmembrane domain of PLB and the Ca-ATPase, since residue Asn^{27} in PLB and Leu^{321} in the Ca-ATPase are near the cytosolic/lipid interface, and Val^{49} in PLB and Val^{89} in the Ca-ATPase are near the luminal interface (*13*, *14*).

Using these constraints, and available high-resolution structures of PLB (1FJK PDB) and the Ca-ATPase (1IWO PDB and 1KJU PDB), two models of the complex between PLB and the Ca-ATPase have been proposed that suggest disruptions in helical elements of PLB are necessary to generate extended structures for PLB that preserve known contact interactions with the Ca-ATPase (*13*, *14*). In the first model of PLB bound to the Ca-ATPase (coordinates provided by Hutter and co-workers as supplementary material in ref *13*), minor disruptions in the helical elements of PLB and positioning of the C-terminus of PLB near the middle of the bilayer are suggested to retain contact interactions between known sites on the cytosolic/lipid interface and cytoplasmic domains of PLB and the Ca-ATPase (Figure 1). In the second model, which takes into account an additional restraint regarding the contact interaction between Val^{49} on PLB and Val^{89} on the Ca-ATPase near the luminal interface (1IWO PDB), much larger disruptions in the secondary structure of PLB are proposed, particularly with respect to residues in domain IB between positions 21 and 31 that are required to become fully extended to bring K^3 in PLB within 15 Å of K^{400} in the crystal structure of the Ca-ATPase (*14*).

Both models permit the cytoplasmic domain of PLB to span much of the 45−55 Å distance apparent in the crystal structure of the Ca-ATPase (1IWO PDB) between known interaction sites on the Ca-ATPase involving Leu^{321} near the cytoplasmic interface and Lys^{400} on the nucleotide binding domain of the Ca-ATPase. However, the apparent spatial separation between sites used for FRET measurements (i.e., Ala^{24} and Tyr^6) in these respective models are approximately 22 Å (*13*) and >30 Å (coordinates not available), which is not consistent with the measured distance (i.e., 14 Å) between these sites (Table 1). Furthermore, prior measurements indicate that upon association with the Ca-ATPase that (i) there are no large changes in the secondary structure of PLB and (ii) the linker region connecting the transmembrane and cytosolic domains of PLB becomes more ordered (*19*, *20*). Rather, PLB binding stabilizes the backbone-fold of the Ca-ATPase, altering the average orientation and amplitude of motion of the nucleotide binding domain, previously implicated as a catalytically important domain motion critical to

Table 2: Rotational Dynamics of PMal Bound to Cys^{24} in PLB[a]

experimental conditions[b]	r_o	g_1r_o	φ_1 (ns)	g_2r_o	φ_2 (ns)	r_∞	χ^2_R[c]
PLB alone	0.31 ± 0.03	0.12 ± 0.01	0.7 ± 0.4	0.10 ± 0.01	14 ± 5	0.09 ± 0.02	6.1
PLB + Ca-ATPase	0.29 ± 0.07	0.10 ± 0.05	0.8 ± 0.6	0.05 ± 0.02	17 ± 6	0.14 ± 0.01	5.0

[a] Mean values and associated standard errors of the mean obtained from a four-exponential fit to frequency-domain data collected for PMal bound to Cys^{24}, as described in the legend of Figure 7. [b] Associated errors were obtained from error surfaces associated with simultaneous fits to three independent measurements obtained from a global fit to three data sets (*46*). [c] Average value of the reduced chi-squared (χ^2_R) fit to a multiexponential decay model.

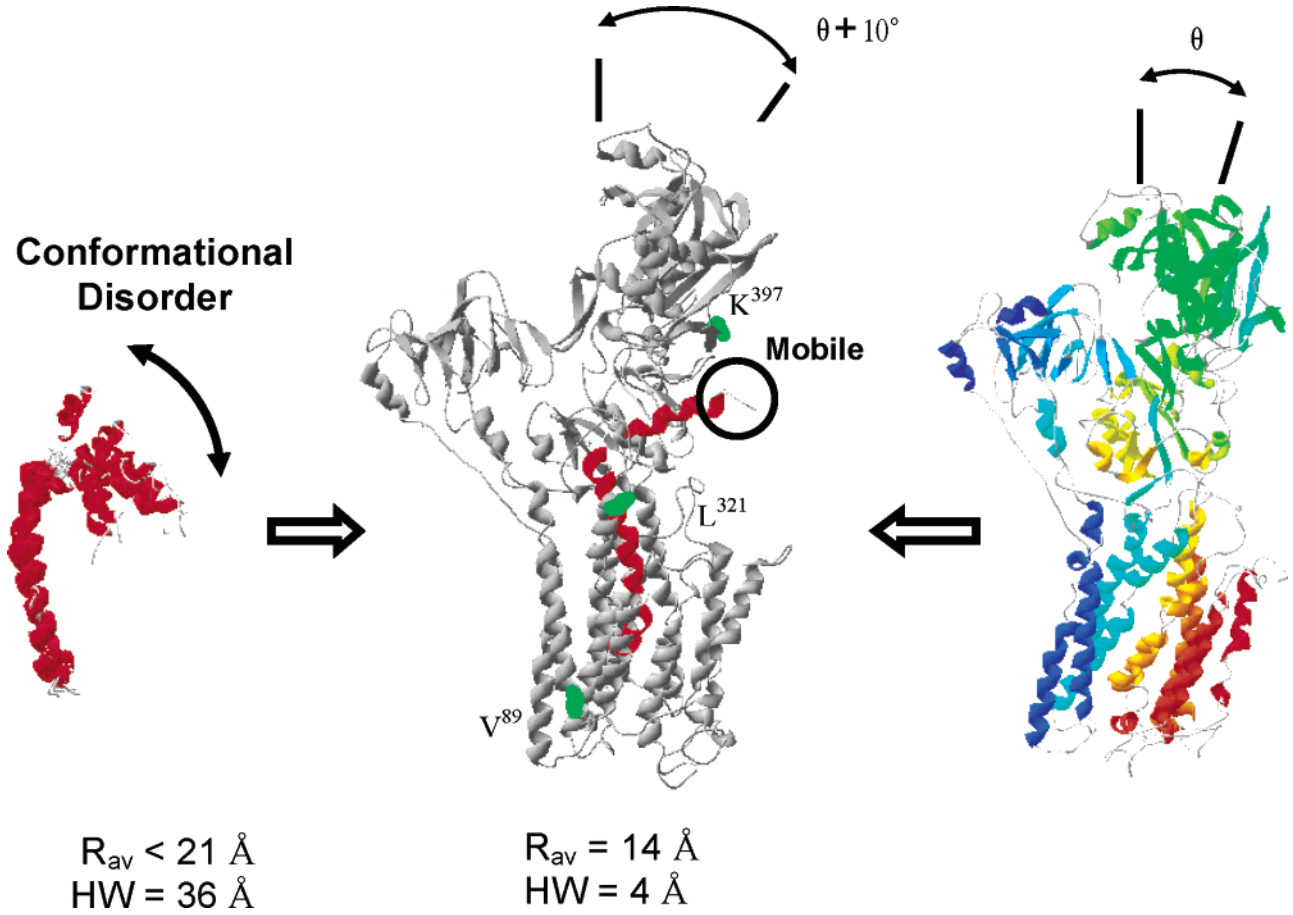

FIGURE 8: Phospholamban binding induces nucleotide domain reorientation. Models depict static disorder (HW = 36 Å) in the cytosolic domain of PLB (left; 1FJP PDB) and the average structure of the apo-form of the Ca-ATPase (right; 1KJU) prior to their association (middle). Following association with the Ca-ATPase, PLB adopts a unique structure (R_{av} = 14 Å; HW = 3.7 Å) that requires the nucleotide binding domain of the Ca-ATPase to undergo a rigid body reorientation, where the average orientation changes by approximately 10°, bringing the binding sequence for PLB into closer proximity of residues near the amino-terminus of PLB with no significant change in the average secondary structure of PLB, as previously measured (*20*, *21*, *49*). Known interaction sites between PLB and Ca-ATPase (shown in green), identified using mutagenesis and chemical cross-linking, are maintained. Specifically, Lys^3 in the cytosolic domain of PLB (known to be rotationally mobile; ref *27*) is located within 15 Å of K^{397} and K^{400} on the nucleotide binding domain of the Ca-ATPase while maintaining contact interactions between the transmembrane sequence of PLB (i.e., N^{27} and V^{49}) and the sites on transmembrane helix M4 of the Ca-ATPase (i.e., L^{321} and V^{89}) (*14*, *50*, *59*). Individual structures of PLB and the Ca-ATPase are derived from PDB coordinates using the program Swiss-PDB viewer (*9*, *61*, *65*).

nucleotide utilization and calcium transport by the Ca-ATPase (*10*, *12*, *20*, *21*, *49*−*57*, *59*, *60*).

Thus, PLB binding induces a reorientation of the nucleotide binding domain toward the bilayer surface, which brings known interaction sites between PLB and the Ca-ATPase into close proximity (Figure 8). Prior results, furthermore, indicate that the dynamics of the nucleotide binding domain correlate with enzymatic function, and their importance in mediating phosphoenzyme formation has been clarified using computer simulations that indicate critical roles for structural flexibility of the cytoplasmic domains of the Ca-ATPase, especially the nucleotide binding domain, in promoting phosphoenzyme formation (*21*, *55*−*62*). These results suggest that PLB functions as an allosteric regulator of the Ca-ATPase by inducing global changes in the orientation and dynamics of the nucleotide binding domain of the Ca-ATPase, resulting in a decreased efficiency of nucleotide utilization and phosphoryl transfer.

Conclusions and Future Directions. Before binding to the Ca-ATPase, the cytosolic domain of PLB assumes a wide range of conformations (Figure 8). Following binding to the Ca-ATPase, the cytosolic domain assumes a unique and homogeneous conformation. No large changes in the backbone structure of PLB occur; rather binding to the Ca-

ATPase selectively stabilizes one conformation of PLB with commensurate changes in the orientation of the nucleotide binding domain of the Ca-ATPase. Thus, PLB binding to the Ca-ATPase inhibits transport activity by restricting catalytically important motions involving the nucleotide binding domain of the Ca-ATPase, which functions to couple ATP hydrolysis to calcium transport. Future measurements should seek to clarify how phosphorylation modulates the precise binding interactions between PLB and the Ca-ATPase to identify the molecular mechanism associated with conformational switching.

REFERENCES

1. Cantilina, T., Sagara, Y., Inesi, G., and Jones, L. R. (1993) *J. Biol. Chem. 268*, 17018−17025.
2. Ferrington, D. A., Yao, Q., Squier, T. C., and Bigelow, D. J. (2002) *Biochemistry 41*, 13289−13296.
3. Bers, D. M. (2001) in *Excitation-contraction coupling and cardiac contractile force*, 2nd ed., Ch. 7, pp 164−169, Kluwer Academic Publishers, Boston.
4. Berridge, M. J., Bootman, M. D., and Roderick, H. L. (2003) *Nat. Rev. Mol. Cell Biol. 4*, 517−529.
5. MacLennan, D. H., and Kranias, E. G. (2003) *Nat. Rev. Mol. Cell Biol. 4*, 566−577.
6. Marx, J. (2003) *Science 300*, 1492−1496.
7. Schmidt, A. G., Kamisago, M., Asahi, M., Li, G. H., Ahmad, F., Mende, U., Kranias, E. G., MacLennan, D. H., Seidman, J. G., and Seidman, C. E. (2003) *Science 299*, 1410−1413.
8. Schwinger, R. H. G., and Frank, K. F. (2003) *Sci. STKE 180*, 15.
9. Lamberth, S., Schmid, H., Muenchbach, M., Vorherr, T., Krebs, J., Carafoli, E., and Griesinger, C. (2000) *Helv. Chim. Acta 83*, 2141−2152.
10. Toyoshima, C., Nakasako, M., Nomura, H., and Ogawa, H. (2000) *Nature 405*, 647−655.
11. Young, H. S., Jones, L. R., and Stokes, D. L. (2001*) Biophys. J. 81*, 884−894.
12. Toyoshima, C., and Nomura, H. (2002) *Nature 418*, 605−611.
13. Hutter, M. C., Krebs, J., Meiler, J., Griesinger, C., Carafoli, E., and Helms, V. (2002) *Chembiochem. 3*, 1200−1208.
14. Toyoshima, C., Asahi, M., Sugita, Y., Khanna, R. Tsuda, T., and MacLennan, D. H. (2003) *Proc. Natl. Acad. Sci. U.S.A. 100*, 467−472.
15. Pollesello, P., Annila, A., and Ovaska, M. (1999) *Biophys. J. 76*, 1784−1795.
16. Pollesello, P., and Annila, A. (2002) *Biophys. J. 83*, 484−490.
17. Li, J., Bigelow, D. J., and Squier, T. C. (2003) *Biochemistry 42*, 10674−10682.
18. Chen, B., and Bigelow, D. J. (2002) *Biochemistry 41*, 13965−13972.
19. Hughes, E., and Middleton, D. A. (2003) *J. Biol. Chem. 278*, 20835−20842.
20. Tatulian, S. A., Chen, B., Li, J., Negash, S., Middaugh, C. R., Bigelow, D. J., and Squier, T. C. (2002) *Biochemistry 41*, 741−751.
21. Negash, S., Chen, L. T., Bigelow, D. J., and Squier, T. C. (1996) *Biochemistry 35*, 11247−11258.
22. Chen, P. S., Toribara, T. Y., and Warner, H. (1965) *Anal. Chem. 28*, 1756−1758.
23. Fernandez, J. L., Rosemblatt, M., and Hidalgo, C. (1980) *Biochim. Biophys. Acta 599*, 552−568.
24. Yao, Q., Chen, L. T., and Bigelow, D. J. (1998) *Protein Expression Purif. 13*, 191−197.
25. Yao, Q., Bevan, J. L., Weaver, R. F., and Bigelow, D. J. (1996) *Protein Expression Purif. 8*, 463−468.
26. Schaffner, W., and Weissmann, C. (1973) *Anal. Biochem. 56*, 502−514.
27. Negash, S., Yao, Q., Sun, H., Li, J., Bigelow, D. J., and Squier, T. C. (2000) *Biochem. J. 351*, 195−205.
28. Yao, Q., Chen, L. T. L., Brungardt, K., Squier, T. C., and Bigelow, D. J. (2001) *Biochemistry 40*, 6406−6413.
29. Lanzetta, P. A., Alvarez, L. J., Reinach, P. S., and Candia, D. A. (1979) *Anal. Biochem. 100*, 95−97.
30. Fabiato, A. (1988) *Methods Enzymol. 157*, 378−417.
31. Haugland, R. P. (2003) in *Handbook of Fluorescent Probes and Research Chemicals*, 9th ed., Molecular Probes, Inc., Eugene, OR.
32. Riordan, J. F., and Vallee, B. L. (1972) *Methods Enzymol. 25*, 515−521.
33. Hunter, G. W., and Squier, T. C. (1998*) Biochim. Biophys. Acta 1415*, 63−76.
34. Haas, E., Katchalski-Katzir, E., and Steinberg, I. (1978) *Biochemistry 17*, 5064−5070.
35. Weber, G. (1981) *J. Phys. Chem. 85*, 949−953.
36. Beechem, J. M., and Haas, E. (1989) *Biophys. J. 55*, 1225−1236.
37. Cheung, H. C. (1991) in *Topics in Fluorescence Spectroscopy* (Lakowicz, J. R., Ed.) Vol. 2, pp 128−176, Plenum Press, New York.
38. Sun, H., Yin, D., and Squier, T. C. (1999) *Biochemistry 38*, 12266−12279.
39. Lakowicz, J. R., Gryczynski, I., Wiczk, W., Kusba, J., and Johnson, M. L. (1991) *Anal. Biochem. 195*, 243−257.
40. Yao, Y., Schoneich, C., and Squier, T. C. (1994) *Biochemistry 33*, 7797−7810.
41. Johnson, M. L., and Faunt, L. M. (1992) *Methods Enzymol. 210*, 1−37.
42. Bevington, P. R. (1969) in *Data Reduction and Error Analysis for the Physical Sciences*, McGraw-Hill, New York.
43. Lakowicz, J. R., and Gryczynski, I. (1991) in *Topics in Fluorescence Spectroscopy* (Lakowicz, J. R., Ed.) Vol. I, pp 293−335, Plenum Press, New York.
44. Kalyanasundaram, K., and Thomas, J. K. (1977) *J. Am. Chem. Soc. 99*, 2039−2044.
45. Sun, H., Yin, D., Coffeen, L. A., Shea, M. A., and Squier, T. C. (2001) *Biochemistry 40*, 9605−9617.
46. Beechem, J. M., Gratton, E., Ameloot, M., Knutson, J. R., and Brand, L. (1991) in *Topics in Fluorescence Spectroscopy* (Lakowicz, J. R., Ed.) Vol. 2, pp 241−306, Plenum Press, New York.
47. MacLennan, D. H., Kumura, Y., and Toyofuku, T. (1998) *Ann. N.Y. Acad. Sci. 853*, 31−42.
48. Wu, P., and Brand, L. (1992) *Biochemistry 31*, 7939−7947.
49. Negash, S., Huang, S., and Squier, T. C. (1999) *Biochemistry 38*, 8150−8158.
50. James, P., Inui, M., Tada, M., Chiesi, M., and Carafoli, E. (1989) *Nature 342*, 90−92.
51. Bigelow, D. J., Squier, T. C., and Thomas, D. D. (1986) *Biochemistry 25*, 194−202.
52. Squier, T. C., and Thomas, D. D. (1988) *J. Biol. Chem. 263*, 9171−9177.
53. Squier, T. C., Bigelow, D. J., and Thomas, D. D. (1988a) *J. Biol. Chem. 263*, 9178−9186.
54. Squier, T. C., Hughes, S. E., and Thomas, D. D. (1988b) *J. Biol. Chem. 263*, 9162−9170.
55. Hunter, G. W., Bigelow, D. J., and Squier, T. C. (1999) *Biochemistry* 38, 4604−4612.
56. Hunter, G. W., Negash, S., and Squier, T. C. (1999) *Biochemistry* 38, 1356−1364.
57. Huang, S., and Squier, T. C. (1998) *Biochemistry 37*, 18064−18073.
58. Toyofuku, T., Kurzydlowski, K., Tada, M., and MacLennan, D. H. (1994) *J. Biol. Chem. 269*, 22929−22932.
59. Jones, L., Cornea, R. L., and Chen, Z. (2002) *J. Biol. Chem. 277*, 28319−28329.
60. Inesi, G., Zhang, Z., and Lewis, D. (2002) *Biophys. J. 83*, 2327−2332.
61. Xu, C., Rice, W. J., He, W., and Stokes, D. L. (2002*) J. Mol. Biol. 316*, 201−211.
62. Li, G., and Cui, Q. (2002) *Biophys. J. 83*, 2457−2474.
63. Fairclough, R. H., and Cantor, C. R. (1978) *Methods Enzymol. 48*, 347−379.
64. Stryer, L. (1978) *Annu. Rev. Biochem. 47*, 819−846.
65. Guex, N., and Peitsch, M. C. (1997) *Electrophoresis 18*, 2714−2723.

BI035424V